

7 Performance analysis of cellular CDMA high-speed 8 data services 9

10 Kevin K. H. Chan¹, Weihua Zhuang^{2*,†} and Young C. Yoon³

11 ¹Qualcomm CDMA Technologies, Qualcomm, Inc., 5775 Morehouse Drive, San Diego, CA 92121, USA

12 ²Centre for Wireless Communications (CWC), Department of Electrical and Computer Engineering, University of
13 Waterloo, Waterloo, Ont., Canada N2L 3G1

14 ³Ericsson Wireless Communications, Inc., 5012 Wateridge Vista Drive, San Diego, CA 92121, USA
15
16
17

18 Summary

19 This paper investigates the forward-link peak and average data rates, throughput, and coverage of a cellular CDMA
20 system for delivering high-speed wireless data services. The analysis takes into account major aspects commonly
21 found in the forward data channel and applies the generalized Shannon capacity formula for multi-element antenna
22 (MEA) systems. The study focuses on the physical layer and is flexible for various propagation environments,
23 antenna configurations, multicode allocations, user distributions, and cell site configurations. Numerical results for
24 various multicode allocations are presented for a system model with two-tier interfering cells operating under a
25 frequency selective slow fading channel with propagation environments specified in the Recommendation ITU-R
26 M.1225. Copyright © 2005 John Wiley & Sons, Ltd.
27
28
29

30
31
32 **KEY WORDS:** code-division multiple access (CDMA) cellular communications; high-speed data service; multi-
33 element antenna (MEA) systems; performance analysis
34
35

36 1. Introduction

37 The interest in the development of wireless high-
38 speed data services is in response to the strong market
39 demand for high-speed wireless internet access.
40 Today's wireless data experience mirrors the wireline
41 experience from the early 1990s. Current wireless
42 data offerings such as short message service (SMS),
43 wireless application protocol (WAP), and i-Mode all
44 suffer from abbreviated interfaces with primarily
45 text-only inputs and low-resolution graphics. Rich
46 media applications typical of today's wireline experi-
47
48
49

ence are not yet widely available in a wireless envi-
50 ronment. It is predicted that wireless systems with
51 enhanced usability and 'killer applications' will
52 most likely follow the astronomical growth rate that
53 wireline systems have experienced [1]. Wireless op-
54 erators and equipment manufacturers are forecasting
55 such a growth rate to occur and this motivates the joint
56 development effort of third-generation (3G) wireless
57 systems, which can support high-speed wireless data.

There exist various standards (such as GPRS,
58 EDGE, cdma2000, cdma2000 1 × EV-DO, cdma
59 2000 1 × EV-DV, HSDPA) for high-speed wireless

*Correspondence to: Weihua Zhuang, Centre for Wireless Communications (CWC), Department of Electrical and Computer Engineering, University of Waterloo, Waterloo, Ont., Canada N2L 3G1.

†E-mail: wzhuang@bcr.uwaterloo.ca

Contract/grant sponsors: Natural Science and Engineering Research Council (NSERC) of Canada; Bell University Research Labs (BUL) at the University of Waterloo.

Table I. High-speed wireless data technologies as of early 2004.

Technologies	Generation	Multiple access	Carrier bandwidth	Peak data rate	Modulation	Data/voice support
GPRS [2,3]	2.5G	Designed as overlay on GSM/TDMA networks TDMA	0.2 MHz	115 kbps	GMSK	Data
EDGE [4]	2.5G	Designed as overlay on GSM/TDMA networks TDMA	2.4 Mbps	384 kbps	8PSK/GMSK	Data
cdma2000 1 × Release 0 [5,6]	3G	CDMA	1.25 Mbps	628 kbps	BPSK/QPSK	Data + voice
IS-856 (1x1;EV-DO, HRD) [7]	3G+	Designed as high data rate extension to cdma2000 CDMA/ TDMA	1.25 Mbps	2.4576 Mbps	QPSK/8PSK/ 16QAM	Data
cdma2000 1x Release D (1xEV-DV) [8]	3G+	Designed as high data rate extension to cdma2000 1 × with voice support CDMA	1.25 Mbps	3.0912 Mbps	QPSK/8PSK 16QAM	Data + voice
UMTS Release 5 (HSDPA) [9]	3G	Designed as high throughput, high peak data rate extension to UMTS Release 99 CDMA	3.84 MHz	1.96 Mbps	QPSK/16QAM	Data + voice

data access. Table I shows a snapshot of high-speed wireless data standards as of early 2004. To evaluate a particular standard, a good approach is to evaluate the channel capacity for such standard deploying in a practical real world scenario. The highest error-free data rate supported in any communication system is well governed by the channel capacity formula. In a perfect noiseless environment where the signal to noise ratio (SNR) is infinite, the channel capacity will be infinite. However, in a real world system, it is not the case. By evaluating users' SNR at various locations and applying the channel capacity formula, one is able to see if the peak data rate advertised in the standard is supported and to what extent it is supported. In addition, the channel capacity 'map' resulting from the operation described above is of great use in coverage analysis and throughput calculation as well. In general, channel capacity, throughput, and coverage are important figures of merit which wireless system engineers require to evaluate the performance of a wireless high-speed data system, to understand the cost advantages and disadvantages of various technologies, and to aid in frequency planning.

Peak data rate is the maximum transmission speed that an individual user may experience in ideal conditions. Since data traffic is bursty in nature, peak data rate affects an individual user's experience. Throughput is the average total capacity available to multiple users within a cell. As throughput increases, each cell site can handle higher volumes of data traffic, and the network requires less equipment and fewer cell sites,

reducing operational expenses and capital investments. Throughput affects both the operator's cost to deliver service and the user's experience. Coverage is the area in which a certain grade of service is guaranteed. As position location technology is required by government regulatory bodies in future wireless operator licensing, it is important to make sure that users located at cell boundaries are still covered with required grade of service.

Before reviewing related work published previously, a few terms should be defined. Multiple input multiple output (MIMO) system refers to a communication system in which multiple transmitting and receiving antennas are deployed. Multiple input single output (MISO) system refers to a communication system in which multiple transmitting antennas and one receiving antenna are deployed. A single input single output (SISO) system refers to a conventional one transmitting antenna and one receiving antenna system. For a MIMO system with n transmitting antennas and n receiving antennas, it has been reported that the system capacity grows at a rate of n bps/Hz for every 3 dB of SNR increase [10], and that the capacity grows linearly with n (referred to as the capacity scaling effect for a MIMO system), assuming independent Rayleigh fading between antenna pairs, fixed total power and bandwidth [11]. In studying the effect of correlation between different MEA subchannels on the capacity scaling effect, it has been shown that the capacity scaling for a MIMO system with n transmitting and n receiving antennas is 10–20% smaller in the presence of correlated fading when

1
2
3 compared to the case of uncorrelated fading [12], and
4 that the *water-filling* algorithm for allocating transmit
5 power among transmitting antennas outperforms
6 equal power distributions [12–14]. It has been argued
7 that the performance of a MISO system can be even
8 worse than a conventional SISO system due to the fact
9 that intracell interference and intercell interference
10 can be enhanced by multi-antenna transmission and
11 multipath channel [15]. A MISO precoder is intro-
12 duced in Reference [15] to attack this problem. In
13 Reference [16], it has been argued that deploying
14 more transmitting antennas than necessary will not
15 enhance capacity.

16 Most of the previous results are obtained by apply-
17 ing the generalized Shannon capacity equation, under
18 the assumption that the received SNR value is a
19 constant value across multiple receiving antennas
20 and only the effects of Rayleigh fading is taken into
21 account. The effects of log-normal fading and dis-
22 tance path loss are ignored. This research attempts to
23 put the capacity expression to work in a real system
24 context. In a real-world system, the SNR at the
25 receiver is affected by the distance path loss, and
26 long-term and short-term fading. The system model
27 used in this research assumes that maximum allow-
28 able power is being transmitted by the transmitter
29 always. It is a valid assumption because in a high-
30 speed wireless system delivering data of bursty nature,
31 transmitting maximum allowable power is of advan-
32 tage from a throughput point of view, as it is the case
33 in the IS-856 air link. As a result, the SNR at the
34 receiver will vary over time due to path loss, shadow-
35 ing, and fading. In addition, with the assumption that
36 the receiving antennas are placed at least half wave-
37 length from each other or any other distance that
38 makes them uncorrelated, each receiving antenna
39 will experience a different channel. Therefore, differ-
40 ent SNR values will appear at different receiving
41 antennas. The numerical results are presented to
42 explore the capacities for various MIMO, MISO,
43 and SISO systems working under different propaga-
44 tion environments. In particular, we analyze the peak
45 and average data rates, throughput and coverage of a
46 cellular code-division multiple access (CDMA) sys-
47 tem for high-speed wireless data delivery in 3G
48 wireless communications. Section 2 describes the
49 cellular CDMA system under consideration, which
50 supports high-speed data. Section 3 presents an ana-
51 lytical model for determining the peak and average
52 data rates, throughput and coverage of the system.
53 Numerical analysis results are presented in Section 4,
54 followed by conclusions in Section 5.

2. System Model

Data services differ fundamentally from voice ser-
vices, noticeably with its bursty nature and high
system resource requirement for the short burst dura-
tion. In addition, data traffic is most likely to appear in
the form of packets. Since a packet has a finite packet
size (or packet duration), a time-division multiplexing
(TDM) multiple access scheme fits well in a packet-
based system.

2.1. Forward Data Channel Structure

Although a TDM based multiple access scheme serves
packet-based services adequately, wireless system
designers still employ Walsh covering as part of the
forward traffic channel. There are several reasons
behind this. First of all, not all packet traffic requires
full system resources. It would be beneficial from
utilization point of view to have a flexible structure so
that the system can decide how much resources to be
allocated to a user. Secondly, it is still expensive to
deploy a carrier for data services only. It would be
ideal for a system to be able to support both high-
speed data services and legacy voice services simul-
taneously. Employing Walsh covering in the forward
traffic channel leads to a very flexible system. Figure 1
shows the block diagram of the forward traffic channel
for the high-speed wireless data system under con-
sideration.

Walsh covering, originally designed to ensure
orthogonality among different users in second-
generation (2G) systems, can be used to provide a
bandwidth on demand platform for flexible system
resource allocation among users. This is the basis of
multicode CDMA [17]. Assume that each Walsh sub-
channel[‡] can deliver data at a certain data rate.
Aggregating more than one Walsh subchannel leads
to a higher data rate. The forward traffic shown in
Figure 1 possesses N Walsh subchannels of a total of
 M subchannels. The rest of the $M - N$ subchannels
can be assigned to different users. The number of
Walsh subchannels assigned to a user can be adjusted
according to the user's QoS requirement and system
resource utilization. The action of assigning more than
one Walsh code to a user is called *code aggregation*.
Since the system can support various data rates, such a

[‡] Note that the concept of Walsh subchannel has nothing to do
with the concept of subchannel in calculating the MEA
system capacity.

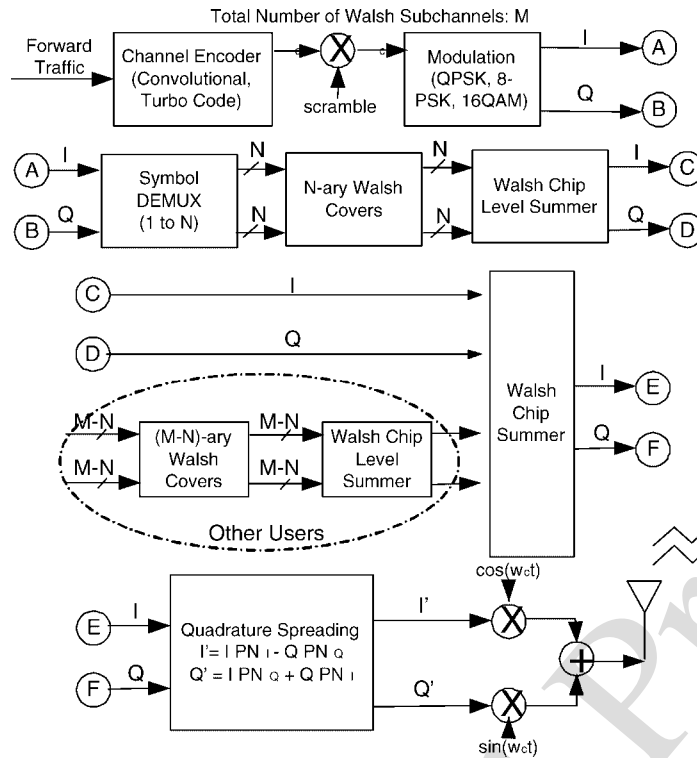


Fig. 1. Simplified forward data channel structure of a wireless system which support high-speed data.

system is also called *multirate CDMA*. Voice services will most likely be assigned with one Walsh subchannel. If a Walsh subchannel can support a data rate higher than the vocoder rate, a Walsh subchannel can be further time-multiplexed to support more than one voice user for packetized voice traffic. There are 16 Walsh subchannels in the IS-856 standard [7, Figure 9.3.1.3.1-1] and 28 assignable Walsh subchannels in the cdma2000 Rel. D standard [8, Table 3.1.3.1.14.4-1].[§]

With such an architecture depicted in Figure 1, the system can support both data users of various data rates and voice users at the same time. If all the Walsh subchannels are assigned to a single user, a time-division multiplexing downlink results. Such a downlink has many benefits: first of all, since the base station only actively serves a user at a time, there will be no intracell interference. Secondly, since there is only one user, the synchronization overhead can be saved. Thirdly, non-data signals such as pilots and control bits can be sent to the target user in advance,

[§]It is noted that the 1xTREM and L3NQS proposals were combined to form IS-2000 Rev. C 1xEV-DV [18].

resulting in 100% of base station power devoted to data delivery. These benefits result into a very good signal quality and this translates to a very high data rate. This is exactly the case for IS-856's forward traffic channel. IS-856's forward traffic channel is a TDM-based downlink and the base station is always transmitting at full power serving one user at a time. On the other hand, if all the codes are assigned to different users, the system can support the maximum number of simultaneously 'on' users. This is ideal if all the users are of voice grades. A mixture of data and voice users can also be supported simultaneously by carefully assigning the number of Walsh subchannels to any particular user.

2.2. Multi-Element Antenna Channel

There are numerous changes in the downlink design philosophy of 3G wireless systems, when compared to 2G systems. These include the introduction of link adaptation, opportunistic scheduling, hybrid ARQ, incremental redundancy, multicode, higher order signal modulation, hard handoff (sector switching), and fast power control [5,19]. The changes result from (a) the lessons learnt from 2G systems, (b) the objective

to increase the utilization efficiency of channel capacity, and (c) the fact that data traffic is fundamentally different from voice traffic. Future breakthroughs in wireless communications will be driven largely by high data rate applications. Sending video rather than speech, for example, requires increasing the data rate by two or three orders of magnitude. Increasing the link or channel bandwidth is a simple but expensive—and ultimately unsatisfactory—remedy. As a result, in a continuing effort to improve system capacity and enhance throughput, researchers around the world have been looking into ways to improve the signal quality under a scattering propagation environment, thus increasing the data rate that a user experiences. The classic approach is to employ antenna diversity, which is believed to be a practical and effective technique for reducing the effect of multipath fading in the wireless propagation environment [20].

In a wireless mobile environment, the fading dispersive channel introduces significant transmission performance degradation. The most effective approach to combating channel fading is to use multiple transmitting and/or receiving antennas and perform combining or selection and switching in order to improve the quality of the received signal. This is the basis of CDMA RAKE receivers, in which each RAKE finger independently tracks a replica of the transmitted signal conveyed by the scattering channel. However, due to space constraint, it is difficult to deploy substantial number of antennas at a mobile handset. In addition, the economy of scale makes it unreasonable to have a large number of antennas on each mobile handset. As a result, multiple antennas at the base station are often deployed. We consider a multi-element antenna (MEA) wireless system [11,13,14], as shown in Figure 2. In the figure, there are n_t transmitting antennas and n_r receiving antennas in the MEA system; s_i is the signal transmitted on the i th transmitting antenna, r_j is the signal received on the j th receiving antenna, and n_j is the additive noise which appears on the j th receiving antenna. As a result, the channel transfer function matrix \bar{H} has a dimension of $n_t \times n_r$, given by

$$\bar{H} = \begin{bmatrix} h_{11} & h_{12} & \dots & h_{1n_r} \\ h_{21} & h_{22} & \dots & h_{2n_r} \\ \vdots & \vdots & \vdots & \vdots \\ h_{n_t1} & h_{n_t2} & \dots & h_{n_tn_r} \end{bmatrix}. \quad (1)$$

Each element of the channel transfer function matrix \bar{H} is assumed to be piecewise-constant over time.

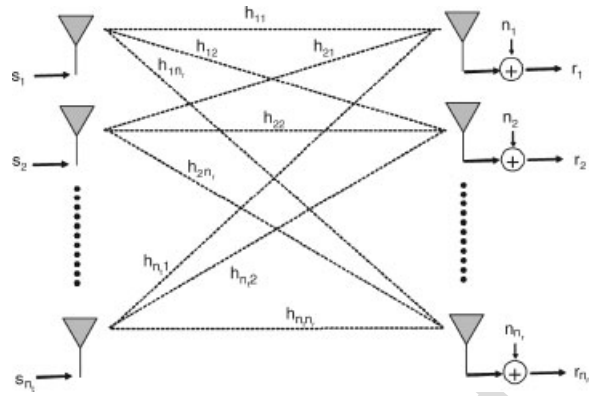
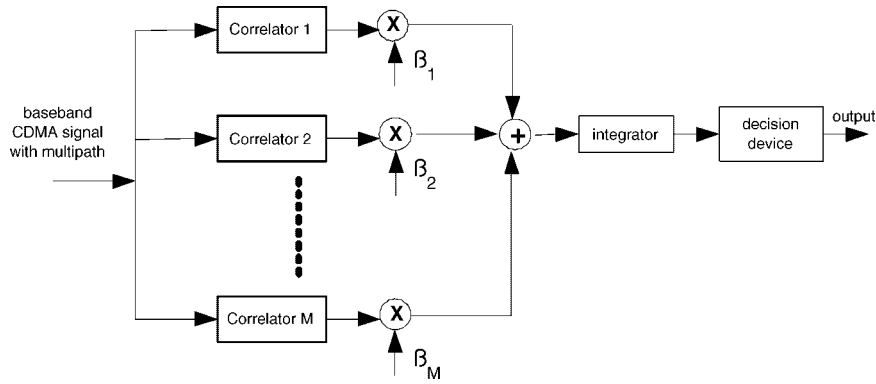


Fig. 2. A multi-element antenna (MEA) system with n_t transmitting antennas and n_r receiving antennas.

We consider a wireless cellular CDMA system with hexagonal cells. The system is fully loaded: all the base stations transmit signals at the maximum allowable power permitted by regulations. This also means that all the base stations are transmitting at the same power level. In the event that more than one transmitting antenna is deployed at each cell site, the total amount of power transmitted remains at the same level as in the case with only one transmitting antenna and the power is divided equally among the transmitting antennas. With a constant transmit power level, the received signals are subject to path attenuation, shadowing, and fading. Here, we use the log-distance path loss with log-normal shadowing, and the tapped-delay line model for frequency-selective fading, as specified in Reference [21] for indoor, outdoor to indoor, and vehicular test environments, respectively. More details of other system level parameters such as cell sectorization, antenna pattern, antenna gain, etc., can be found in References [22,23].

2.3. RAKE Receiver

The receiver structure plays an important role in the calculation of the SNR. In addition to the receiver structure, the combining strategy can also affect the output SNR of the receiver. The RAKE receiver is the most commonly used receiver structure in CDMA systems. A RAKE receiver attempts to collect time-shifted versions of the original transmitted signals by providing a separate correlation receiver for each of the multipath signals. Figure 3 shows an L -finger RAKE receiver. The RAKE receiver utilizes multiple correlators to separately detect the L strongest multipath components. The outputs of each correlator are weighted to provide a better estimate of the

Fig. 3. An L -finger RAKE receiver.

transmitted signal than is provided by a single component. In Figure 3, $\beta_l, l = 1 \dots L$, are the weights assigned to each of the finger. The strategy, which assigns weights to the fingers is called combining strategy. Demodulation and bit decisions are then based on the weighted outputs of the L correlators.

There are several linear combining strategies available, such as selective diversity combining, maximal ratio combining (MRC), and equal gain combining. MRC assigns weights to each of the finger by its corresponding channel gain conjugate. Maximal ratio combining achieves the highest SNR at the combiner output by coherently combining all the signals from the L fingers and by assigning a larger weight to a signal component with better quality [24]. A RAKE receiver employing MRC is considered in this study. The average SNR at the output of the MRC combiner is simply equal to the sum of the individual average SNR from the correlator output of each finger [25, p128]. For the system deploying multiple receiving antennas (i.e., $n_r > 1$), it is assumed that each of the receiving antenna has its own RAKE receiver employing MRC. By means of that, each receiver has its own output SNR, which is used to compute channel capacity bounds.

3. Data Rate, Throughput, and Coverage

3.1. Throughput and Capacity Bound

We study both peak data rate and average data rate. The former is the maximum transmission speed that an individual user may experience in ideal conditions, while the latter is the data rate that a user can achieve on the average. Coverage is the area in which a certain grade of service is guaranteed. A cell is said to be

covered when a pre-defined minimal grade of service is guaranteed throughout the whole cell, especially area which is close to cell boundaries. Wireless network operators want their cells to be fully covered always. In addition, wireless network operators may also want to find out the percentage of area in which a certain grade of service can be provided. The coverage map is of great use here. Using the average data rate is more appropriate in evaluating coverage than using the peak data rate. Throughput of a cell is the total amount of data rate available to multiple users within a cell for a given period of time. From a physical layer point of view, peak cell throughput can be obtained by integrating the peak data rate distribution across the cell coverage area, scaled by the user distribution. Similarly, average cell throughput can be obtained by integrating the average data rate distribution across the cell coverage area, scaled by the user distribution. The peak or average cell throughput $t_{p_{\text{peak,avg}}}$ is given by

$$t_{p_{\text{peak,avg}}} = \frac{4}{2.598R^2} \left[\int_0^{R/2} \int_0^{R\sqrt{3}/2} f_d(x,y)f_c(x,y)dydx + \int_{R/2}^R \int_0^{\sqrt{3}(R-x)} f_d(x,y)f_c(x,y)dydx \right] \quad (2)$$

where (x, y) is the mobile location coordinates, $f_d(x, y)$ is the peak or average data rate value at the mobile location, $f_c(x, y)$ is the probability density function (pdf) of the geographical user location. The throughput is averaged over a hexagonal cell with area $2.598R^2$.

Based on the generalized Shannon capacity formula, the capacity lower bound, C , for a combined

transmit and receive diversity MEA system is given by [10]^{Q2}

$$C > \sum_{k=n_t-(n_r-1)}^{n_t} \log_2 [1 + \{(\rho_k/n_t) \times \chi_{2k}^2\}] \quad (3)$$

where ρ_k is the average SNR at the k th receiving antenna, and χ_{2k}^2 is the central Chi-square random variable with $2k$ degrees of freedom corresponding to the channel gain square in a Rayleigh fading environment. Equation (3) can be interpreted as follows. Since there are multiple transmit and receiving antennas, there are multiple subchannels between the transmitter and the receiver. Under the assumption of uncorrelated scattering, the total MEA system capacity is the sum of capacities of the subchannels. The number of subchannels available between the transmitter and receiver is determined by the number of transmit and receiving antennas, as indicated in the summation indices in Equation (3). In addition, each of the subchannel provides *two or multiple of two degrees of diversity*, as given by the Chi-square random variable with two or multiple of two degrees of freedom. The two degrees of diversity come from the fact that there are real and quadrature components in the elements of the channel transfer function matrix. Since the total capacity is the sum of individual subchannel capacity, an MEA system can deliver an increase in capacity when compared to system with only one transmitting and one receiving antenna.

3.2. Calculation of SNR

In calculating the average SNR value in Equation (3), the effect of propagation path attenuation should be considered, and the interference sources include intercell interference, intracell interference, interchip interference, interpath interference, and ambient noise.

To compute the received signal power and interference power at any location within a cell, the effect of the large scale path loss and shadowing should be taken into account. ITU-R M.1225 Recommendation [21, Section 1.2.1] provides the equations of mean path loss (in dB) for the three test environments under worst case propagation, given by

$$L(r, f) = \begin{cases} 37 + 30 \log_{10} r + 18.3n^{((n+2)/(n+1))-0.46} & \text{(indoor)} \\ 40 \log_{10} r + 30 \log_{10} f + 49 & \text{(outdoor to indoor and pedestrian)} \\ 40(1 - 4 \times 10^{-3} \Delta h_b) \log_{10} r - 18 \log_{10} \Delta h_b + 21 \log_{10} f + 80 & \text{(vehicular)} \end{cases} \quad (4)$$

where r is the transmitter-receiver separation in metres for the indoor environment and in kilometers for the other environments, n is the number of floors in the propagation path, Δh_b is the antenna height in metres, and f is carrier frequency in MHz. The shadowing is usually modeled by a log-normal distribution.

3.2.1. Received signal power

The forward link uses multicode CDMA to provide a bandwidth on demand platform for flexible resources allocation to different users within a cell. By aggregating more Walsh subchannels to a user, the user will get more system resources and a higher data rate. On the other hand, the level of intracell interference that a user experiences depends on the number of remaining Walsh subchannels not assigned to that particular user. For a multiuser power limited wireless communication system, allocating more Walsh subchannels to a user is equivalent to allocating more power to that particular user [26, Section III-B]. Let S_T denote the total transmit power at the base station. Under the assumption that the transmitter power is distributed equally among all the M identical Walsh subchannels, each subchannel has a power of S_T/M . A user allocated with N of M Walsh subchannels has an overall data rate N times the data rate of each subchannel. A user who possesses more than one Walsh subchannel will not incur *self interference*. Since the user's Walsh subchannels are created from the same codebook and they are delivered through the same physical medium, they are orthogonal to each other by default.

Since the output SNR of a RAKE receiver is the sum of SNR on each of the RAKE finger, a power weight can be introduced to describe the signal power received on a particular RAKE finger. The power weights of all the fingers are given in the channel profile of the operating environment [21]. Let the power weight of the i th RAKE finger be p_i , the power received on the i th RAKE finger is therefore

$$S_{R,i} = \frac{p_i S_T 10^{-L(r_0, f)/10} 10^{-\xi_0/10}}{M} \quad (5)$$

where r_0 is the distance between the mobile user and its serving base station, ξ_0 is a zero-mean Gaussian

Table II. Standard deviations of log-normal distributed random variables (ξ, ξ_0) for the three test environments [21].

Test environment	Standard deviation σ_{ξ, ξ_0} dB
Indoor	12
Outdoor to indoor and pedestrian (users located outdoor)	10
Outdoor to indoor and pedestrian (users located indoor)	12
Vehicular	10

random variable with the standard deviation in dB given in Table II. A statistical average can then be taken with respect to the random variable to obtain a constant average received power for each mobile user location.

3.2.2. Interpath interference (IPI)

Baseband waveshaping filtering, also referred to as chip pulse shaping, has a significant impact on interpath interference (IPI) and interchip interference (ICI). IS-95, cdma2000, and all high data rate extensions of cdma2000 use baseband waveshaping filters designed to meet a bandwidth constraint while minimizing intersymbol interference (ISI) or interchip interference. A figure of merit which has an impact on IPI is the total duration of the waveshaping filter's impulse response. With a chip rate of 1.2288 Mcps, an IS-95 waveshaping filter is time-limited to a duration of $12T_c$ [27, p60], where T_c is the chip duration 813 ns. With the IS-95 waveshaping filter, assuming the l th RAKE finger is placed at time τ_l and the i th multipath appears at time τ_p , if $|\tau_l - \tau_p| < 6T_c$,[¶] then the l th RAKE finger will capture power from the i th multipath. Otherwise, the i th multipath will not contribute any signal power to the RAKE finger and the power delivered through that multipath will become interference. This type of interference is generalized as IPI [28, Section 3]. Since the power weight of the i th multipath is p_i , the sum of IPI power which appears on the i th multipath will therefore has a weight of $1 - p_i$. With the transmitter power S_T and a total of M Walsh subchannels, a user located at a distance r_0 from the base station operating at a frequency f will received an IPI power equals to

[¶]The waveshaping filter impulse response spans from $-6T_c + \tau_p$ to $6T_c + \tau_p$.

$$\mathcal{I}_{\text{IPI}} = \frac{(1 - p_i)S_T 10^{-L(r_0, f)/10} 10^{-\xi_0/10}}{M} \quad (6)$$

3.2.3. Intercell interference

One of the distinctive features of cellular CDMA system is universal frequency re-use. All the cells within the coverage area operate at the same carrier frequency. As a result, transmission performance of the target user is degraded by intercell interference resulting from transmissions in all other cells. The interference power is the sum of the received power levels from all other cells in the system. Taking into account the log-normal shadowing, the sum of independent log-normal random variables is required and the procedure of obtaining such sum is described in Reference [29]. For simplicity, assuming no shadowing, the intercell interference is given by

$$\mathcal{I}_{\text{inter}} = \sum_{n=1}^{\infty} S_T 10^{-L(r(x, y|n), f)/10} \quad (7)$$

where $r(x, y|n)$ is the distance between the n th interfering base station and the target user, and (x, y) is the target user's coordinates.

3.2.4. Intracell interference

In the CDMA system, multiuser support is accomplished through the use of Walsh subchannels. Each Walsh subchannel is designed to be orthogonal to each other. In the ideal case in which the propagation characteristics of wireless channels used by different users are the same, there will be no intracell interference. It is because interference will be completely eliminated by orthogonal Walsh covers. In reality, users request services at different time. If the time between service requests is greater than the channel coherence time, the users experience different propagation characteristics on their wireless channels. Hence, the Walsh covers no longer are orthogonal to each other and users experience interference (referred to as intracell interference) from other transmissions in the same cell. Under the assumption that the system is fully loaded, if the target user is assigned with N ($< M$) Walsh subchannels, the rest of the $(M - N)$ Walsh subchannels will be assigned to other users. With a total transmitted power of S_T and an operating frequency of f , a user who is located at r_o from the

base station will experience an intracell interference power of

$$\mathcal{J}_{\text{intra}} = \frac{\zeta(M - N)S_T 10^{-L(r_o, f)/10} 10^{-\xi/10}}{M} \quad (8)$$

where $\zeta \in [0, 1]$ is an orthogonal factor [30,31]; ξ is an iid random variable with respect to ξ_0 whereas its standard deviation in dB is given in Table II. The orthogonal factor is used to capture the fact that Walsh coverings, in some cases, may be orthogonal to each other. For example, for line-of-sight (LOS) communication with no multipath, an orthogonal factor of zero can be used. For a worst case analysis, an orthogonal factor equals to 1 can be used. In this research, we adopt a worst case analysis (i.e., $\zeta = 1$).

3.2.5. Interchip interference (ICI)

As shown in Figure 1, signals on the forward link will go through a quadrature spreading block. The quadrature spreading block will apply a pseudorandom spreading sequence to the incoming signal, as well as a waveshaping pulse designed to meet a bandwidth constraint and minimize interference to other signals.^{||} In some cases described below, the receiver's current chip window will unintentionally capture power from the previous chips and future chips. ICI refers to the power spilled from the previous chips and future chips into the current chip.

Obviously, the design of the waveshaping pulse has a direct relationship with ICI. If the autocorrelation function of the waveshaping pulse does not satisfy the Nyquist criterion, interchip interference will occur [32]. Autocorrelation function is used here because SNR maximizing receivers such as the matched filter receiver use the same waveshaping pulse as the transmitter to derive their output statistics. The other scenario in which ICI occurs is the receiver's imperfectness in tracking the incoming paths.

First, the autocorrelation function of the chip waveforms is required. Letting $g(t)$ be the time domain representation of the chip waveform satisfying $\int_{-\infty}^{\infty} |g(t)|^2 dt = 1$, the autocorrelation function of the chip waveform $\hat{g}(t)$ is given by

$$\hat{g}(t) \equiv g(t) \star g^*(-t) \equiv \int_{-\infty}^{\infty} g(t + \tau)g(\tau)d\tau \quad (9)$$

^{||}The waveshaping pulse is not shown in Figure 1.

where \star is the convolution operator and $*$ is the complex conjugate operator. It is interesting to note that $\hat{g}(0) = 1$. Since any autocorrelation function is maximum at its origin, $\hat{g}(t) \leq 1$. Considering only the waveshaping pulse and neglecting any propagation effect, if the receiver perfectly tracks the incoming path, the average power of the receiver's output equals to $|\hat{g}(0)|^2$ [33].

Consider the case where the autocorrelation function of the waveshaping pulse does not satisfy the Nyquist criterion, the user will receive an interference power $\mathcal{J}_{\text{ICI}_1}$ given by

$$\mathcal{J}_{\text{ICI}_1} = S_{R,i} \sum_{l=-\infty, l \neq 0}^{\infty} |\hat{g}(lT_c)|^2 \quad (10)$$

Consider the case where there is a difference of τ_o between the time that the receiver places its receiving finger and the time that the incoming multipath appears, the interference power $\mathcal{J}_{\text{ICI}_2}$ can be described by

$$\mathcal{J}_{\text{ICI}_2} = S_{R,i} (1 - |\hat{g}(\tau_o)|^2) \quad (11)$$

and a factor of $|\hat{g}(\tau_o)|^2$ has to be introduced to Equation (5) in order to correctly reflect the fact that the receiver receives less signal power than the perfect tracking case. For the case where the waveshaping pulse does not satisfy the Nyquist criterion and there exists incoming path tracking errors, Equation (10) becomes

$$\mathcal{J}'_{\text{ICI}_1} = S_{R,i} \sum_{l=-\infty, l \neq 0}^{\infty} |\hat{g}(lT_c + \tau_o)|^2 \quad (12)$$

The total ICI power the user receives in this case is the sum of $\mathcal{J}'_{\text{ICI}_1}$ and $\mathcal{J}_{\text{ICI}_2}$.

The tracking error τ_o can be described as a random variable which is uniformly distributed from $[0, T_c]$. The average ICI power in the presence of tracking errors is therefore

$$\mathcal{J}_{\text{ICI}_{\text{avg}}} = E[\mathcal{J}'_{\text{ICI}_1} | \tau_o] + E[\mathcal{J}_{\text{ICI}_2} | \tau_o] \quad (13)$$

where $E[\cdot]$ is the expectation operator.

It should be mentioned that: (1) in addition to tracking errors in timing, there exists tracking errors in the signal phase as well. Phase tracking errors do not have any influence on the signal and interference power levels. It is because the power of any phase

errors $e^{-j\theta_n}$ equals to 1; (2) ISI is a special case of ICI. Similar to the definition of ICI, ISI refers to the power spilled from the previous symbols and future symbols into the current symbol interval. It is easy to picture that Equation (13) takes care of ISI; (3) an IS-95 chip waveform is time-limited to $12T_c$. By means of that, the summation range of $-\infty$ to ∞ used in Equations (10) and (12) can be changed to a range of $-11T_c$ to $11T_c$.

In summary, taking into account all the interference sources, given the user is located at coordinate (x, y) , which is at distance r_o from the serving base station, with N of a total of M Walsh subchannels and operating at frequency f with transmit power S_T , the signal power to noise power ratio of i th RAKE finger, ρ_i , for that particular user is

$$\rho_i = \frac{S_{R,i}}{\mathcal{I}_{\text{IPI}} + \mathcal{I}_{\text{inter}} + \mathcal{I}_{\text{intra}} + \mathcal{I}_{\text{ICI}_{\text{avg}}} + N_0} \quad (14)$$

where N_0 is one-sided power spectral density of the background additive white Gaussian noise. Let q denote the number of fingers in the RAKE receiver. By summing $\rho_i, i = 1 \dots q$, the output SNR of the antenna can be obtained. By substituting the output SNRs of the receiving antennas into Equation (3), the peak and average data rates at any location within a cell can be found. Once the peak or average data rate is found for any location, peak or average cell throughput $tp_{\text{peak}}, tp_{\text{avg}}$ can be found using Equation (2). Coverage of a cell can be found by observing the average data rate distribution throughout the cell.

4. Numerical Results

Consider a target cell with intercell interference coming from the first two tiers of the neighboring cells (i.e., there are total 18 interfering cells). The system is located on a flat terrain and all the cells have the same size with cell radius $R = 5$ km for the vehicular and outdoor to indoor environments and $R = 50$ m for the indoor environment. Mobile user location is assumed to be uniformly distributed over the service area.

Numerical results for the downlink is obtained through the application of MEA system lower bound given in Equation (3) and the SNR expression given in Equation (14). There are several random variables in the overall capacity expression, namely the k Chi-square random variables with $2k$ degrees of freedom in Equation (3), the log-normal random variables (characterizing the shadowing phenomenon in the

wireless channel) in the SNR calculation, and the uniformly distributed user location. Each of the random variable is instantiated 100 000 times according to its corresponding distribution. There are 100 000 SNR and capacity samples for each location. The 99 percentile capacity is taken as the peak data rate and the 50 percentile capacity is taken as the average data rate. Peak and average spectral efficiency values are calculated by dividing the peak or average data rate by the bandwidth, respectively. For the vehicular and outdoor to indoor pedestrian channels, new SNR and capacity values are computed for every 100 m along the x-axis and y-axis and these two values are assumed to remain the same for the 100×100 m area. In order to accomplish the worst case analysis and be conservative, the lowest data rate within the 100×100 m area is used in Equation (2) to compute the peak and average throughputs. For the indoor channel, new SNR and capacity values are computed for every 1 m along the x-axis and y-axis and these two values are assumed to be constant for the 1×1 m area. The lowest data rate within the 1×1 m area is used. For the frequency-selective slow fading channel models of ITU-R M.1225, the RAKE receiver is assumed to have three fingers tracking the three strongest paths from the multipath channel. The system has an overall bandwidth of 1.25 MHz centered at 2 GHz and can support a maximum of 28 multicode channels. The antenna height is 15 m for an outdoor environment. For simplicity, ICI is neglected in the SNR calculation. Note that, for systems with large spreading factor, it is shown [34, pp 339–342] that ICI is dwarfed in comparison with the intracell interference. A summary of forward system level simulation parameters used in this study is presented in Table III.

4.1. System Supporting Data User in TDM Mode

Consider that the base station allocates all the resources to only one user at any time. The base station does so by allocating all its multicode channels to that particular user for a specific duration. (Multiple users are supported via TDM.) Since there is only one user at a time, there is no power sharing among users and no overhead power required for synchronization. In addition, there is no intracell interference. As a result, the best possible signal quality is provided to the user. Such a system achieves the highest peak data rate and cell throughput and provides the best coverage. This configuration is good for finding the best operating performance of a wireless system optimized for data.

Table III. Downlink system level simulation parameters.

Parameter	Value	Comments
Number of cells	19	Two rings hexagonal, non-sectorized
Antenna horizontal pattern	Omnidirectional	
Antenna orientation	No loss assumed in the vertical azimuth	
Propagation model	See Equation (4)	Two floors in the propagation path (indoor), 15 m antenna height (vehicular)
Terrian	Flat	
Log-normal shadowing	Standard deviation = 12 dB (indoor, outdoor to indoor, and pedestrian), standard deviation = 10 dB (vehicular)	
Cell radius	50 m (indoor), 5 km (outdoor to indoor and pedestrian, vehicular)	
Site to site distance	86.6 m (indoor), 8.66 km (outdoor to indoor and pedestrian, vehicular)	
Delay spread model	See [21]	
User distribution	Uniform	
Scheduling algorithm	Round robin	
Base station transmit power	500 W	Cell is fully loaded; constant transmit power
MS noise temperature	297 K	
Carrier frequency	2 GHz	
Bandwidth	1.25 MHz	
Number of transmit Antennas (BS)	1–4	BS power divides equally among the antennas
Number of receive antennas (MS)	1–4	
MS receiver	3-finger RAKE on each of the receiving antenna	Maximum ratio combining
Antenna separation	At least half wavelength	Antennas are uncorrelated
Orthogonal factor (ζ)	1	See Equation (8)
Total number of multicode channels	28	
Overhead channel downlink power usage	0%	TDM forward link, overhead is sent in advance

For $n_t = 1$ and $n_r = 2$, Figures 4–6 show: (a) a surface plot of the 50 percentile capacity and (b) the coverage map over one quarter of the hexagonal cell, and (c) the peak and average data rates along the x-axis, respectively, for a data user operating under the ITU-R M.1225 vehicular channel model. Table IV summarizes the key parameters, peak data rate in Mbps, peak throughput in Mbps, average throughput in Mbps, peak spectral efficiency in bps/Hz, and average spectral efficiency in bps/Hz, for the ITU-R M.1225 vehicular channel, outdoor to indoor and pedestrian channel, and indoor channel.

From Figures 4–6 and Table IV, it is observed that: (a) the peak data rate, peak throughput, and peak spectral efficiency are surprisingly good when the system devotes its full resources to a particular user. It should be noted that the peak values shown are theoretical maximum values. In most of the cases, these values cannot be realized in a real world system because of (i) limited SNR due to multipath and simple receiver, (ii) channel fading, (iii) signaling

overheads, (iv) imperfect link adaptation, and (v) practical channel coding and modulation schemes. The $1 \times$ EV-DO field trial results indicate 2.5 Mbps to 4 Mbps average throughput [18]; (b) since the system devotes all the bandwidth resources to only one user, the user will achieve good SNR, especially for the case when the user is located very close to the base station. A good SNR will deliver very high data rates; (c) there can be more than 10 times difference between the average data rates close to the base station and that close to the cell boundary. In other words, the data rates supported by the wireless channel drop dramatically as the user moves away from the base station; (d) we should pay more attention to the average values, especially to the lower bound of the average spectral efficiency. For example, the lower bound of the average spectral efficiency for the outdoor to indoor pedestrian channel is just 0.6 bps/Hz. A 1.25 MHz bandwidth can only deliver a data rate of 750 kbps. User who requests a data rate higher than 750 kbps cannot be guaranteed services all the time.

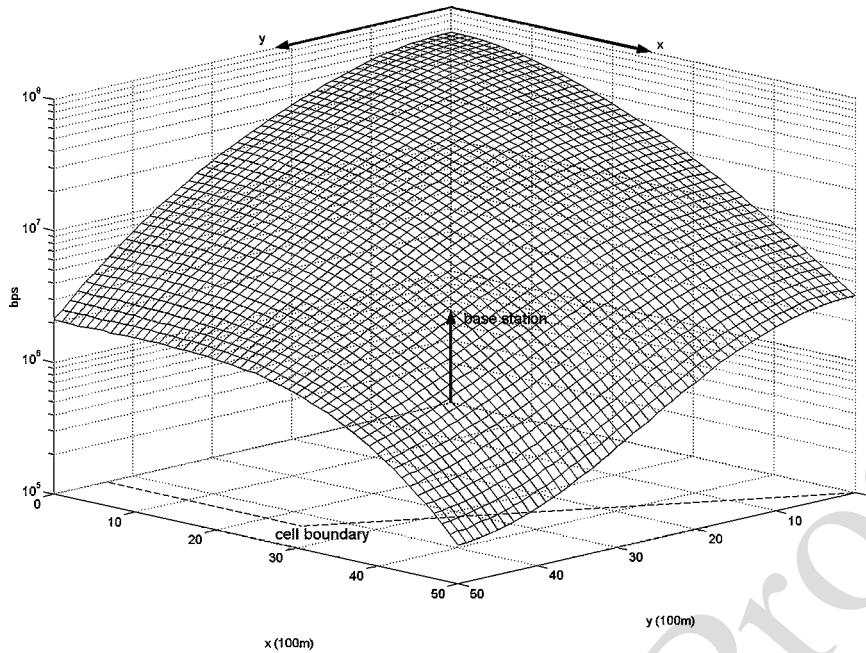


Fig. 4. Downlink coverage map for a data user operating under ITU-R M.1225 vehicular channel model, $n_t = 1, n_r = 2$ (28 multicode channels per user).

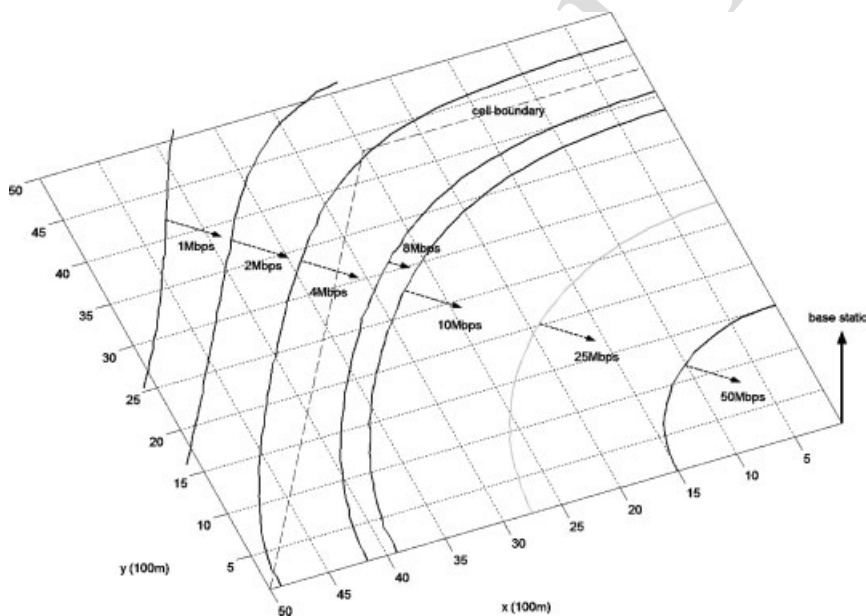


Fig. 5. Downlink coverage map for a data user operating under ITU-R M.1225 vehicular channel model, $n_t = 1, n_r = 2$ (28 multicode channels per user). Q7

4.2. System Supporting Maximum Number of Users

Consider the system designed to support a maximum number of users. The system does so by allocating

only one multicode channel to a particular user at a time. Users will suffer from intracell interference. Such configuration is aimed to support voice users and low data rate users. Numerical results obtained under such configuration is good for finding the worst

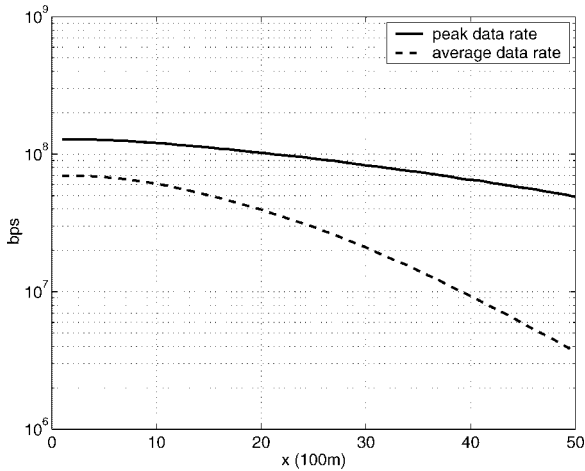


Fig. 6. Downlink peak and average data rates of a data user operating under ITU-R M.1225 vehicular channel model along the x-axis, $n_t = 1, n_r = 2$ (28 multicode channels per user).

case performance of a wireless system optimized for data services. Worst case performance data are important. For example, wireless operators will need to know if a user devoted with minimal resources located at the cell edge is still guaranteed with a certain grade of service.

For $n_t = 1$ and $n_r = 2$, Figures 7 and 8 plot: (a) the coverage map and (b) the peak and average data rates along the x-axis for a data user assigned with a single multicode channel in the vehicular environment. Table V summarizes the key parameters.

From the coverage map, it is shown that high data rates can still be delivered to users located at cell boundaries. The system is able to deliver an average data rate of approximate 70 kbps to users located at cell boundaries in all the three propagation environments. Since a typical vocoder has a code rate of 9.6 kbps to 14.4 kbps, a multicode channel can

Table IV. Downlink performance: 28 multicode channels per user.

Channel	Peak data rate (Mbps)	Peak throughput (Mbps)	Average throughput (Mbps)	Peak spectral efficiency (bps/Hz)	Average spectral efficiency (bps/Hz)
Vehicular	128.5	74.9	20.8	35.9–102.8	2.2–55.6
Outdoor to indoor and pedestrian	11.4	8.5	2.6	6.4–9.1	0.6–6.4
Indoor	125.1	83.1	17.7	55.7–100.1	3.9–50.3

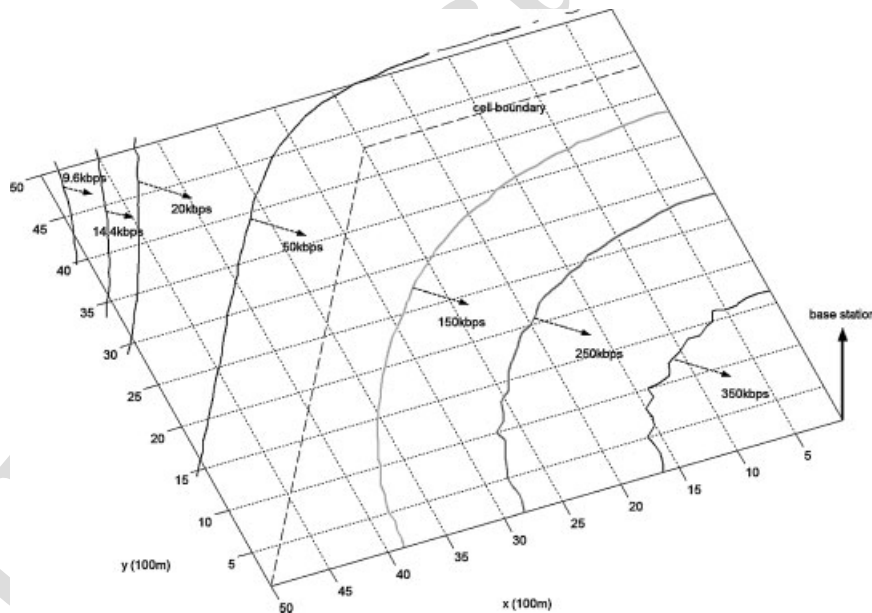


Fig. 7.^{Q7} Downlink coverage map for a voice user operating under ITU-R M.1225 vehicular channel model, $n_t = 1, n_r = 2$ (1 multicode channel per user).

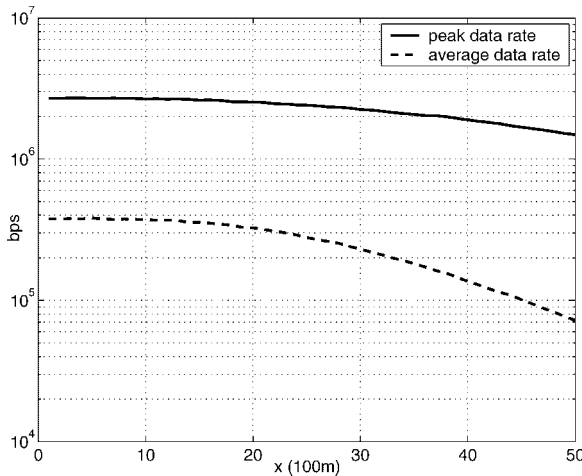


Fig. 8. Downlink peak and average data rates of a voice user operating under ITU-R M.1225 vehicular channel model along the x-axis, $n_t = 1, n_r = 2$ (1 multicode channel per user).

literally support about five voice users in a TDM fashion. As the simulation results are obtained with a total of 28 multicode channels, up to 140 voice users can be supported simultaneously under the assumed configurations.

4.3. Multicode Allocation and its Improvement on Average Data Rate

It is an interesting topic to investigate the performance improvement as more multicode channels are allocated to a particular user. Figure 9 shows the average data rate for a user operating under the ITU-R M.1225 vehicular channel along the x-axis with various multicode allocations of a total of 28 multicode channels. It is observed that the more multicode channels are allocated to a user, the better the average data rate is available to the user. Doubling the number of multicode channels allocated to a user will result into more than doubling the available

average data rate. It is because doubling the number of multicode channels allocated to a user not only allows the user to receive data in parallel, but also reduces intracell interferences. As a result, significant improvement on achievable data rates is observed. This is probably a reason that the forward link of the IS-856 system operates in a TDM fashion.

4.4. System with Multiple Transmitting and Receiving Antennas

Different transmitting and receiving antenna configurations and their impacts on the system capacity are explored in the following numerical analysis. The ITU-R M.1225 vehicular channel is used and results are presented along the x-axis. The user is assumed to possess all the multicode channels. Figure 10 shows the 50 percentile capacity for $n_t = n_r = n, n = 1, \dots, 4$. It is shown that the capacity does not increase linearly with n . However, the capacity does increase when more transmitting and receiving antennas are deployed. Figure 11 shows the average data rates for a receive diversity only system. It shows that deploying more receiving antennas enhances the average data rate. Diminishing return is observed: the more receiving antennas are deployed, the less gain in data rate results. Figure 12 shows the average data rates for a transmit diversity only system. It is shown that deploying multiple transmitting antennas enhances the average data rate. However, the return of deploying multiple transmitting antennas is not as good as deploying multiple receiving antennas, similar to the observations given in Reference [16]. These can be explained as follows: since it is assumed that the total power is kept constant regardless of the number of transmitting antennas, MEA subchannels created by the multiple transmitting antennas will have less power allocated to them, as shown by the n_t factor in Equation (3). Although the degree of diversity of each subchannel increases with the number of transmitting antennas, since the

Table V. Downlink performance: 1 multicode channel per user.

Channel	Peak data rate (Mbps)	Peak throughput (Mbps)	Average throughput (Mbps)	Peak spectral efficiency (bps/Hz)	Average spectral efficiency (bps/Hz)
Vehicular	2.7	2.0	0.2	1.1–2.2	0.05–0.3
Outdoor to indoor and pedestrian	4.6	3.3	0.3	2.2–3.7	0.06–0.7
Indoor	3.3	2.6	0.3	1.8–2.7	0.08–0.6

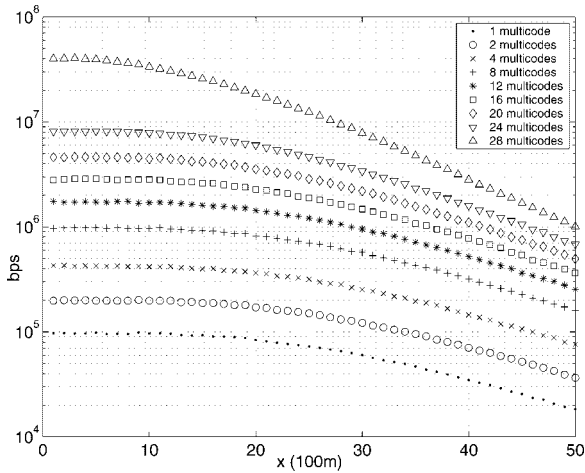


Fig. 9. Downlink average data rate of a user with various multicode allocations of a total of 28 multicodes operating under the ITU-R M.1225 vehicular channel along the x-axis, $n_t = 1, n_r = 1$.

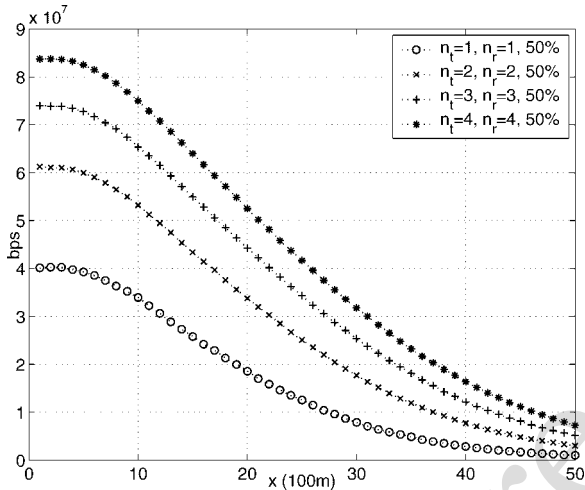


Fig. 10. Downlink average data rate of an MEA system along the x-axis ($n_t = n_r$).

signal quality ultimately determines the channel capacity, the overall benefit of deploying multiple transmitting antennas is not as great as deploying multiple receiving antennas. Figure 13 shows the average data rate for various transmit and receive diversity configurations. Together with numerical results for other diversity configurations, it is observed that for a system which deploys receive diversity, deploying only one transmitting antenna will result in the best average data rates in most cases. Since there is already receive diversity which exploits the rich nature of a multipath channel, there is no need to deploy multiple transmitting antennas. With the constant total power

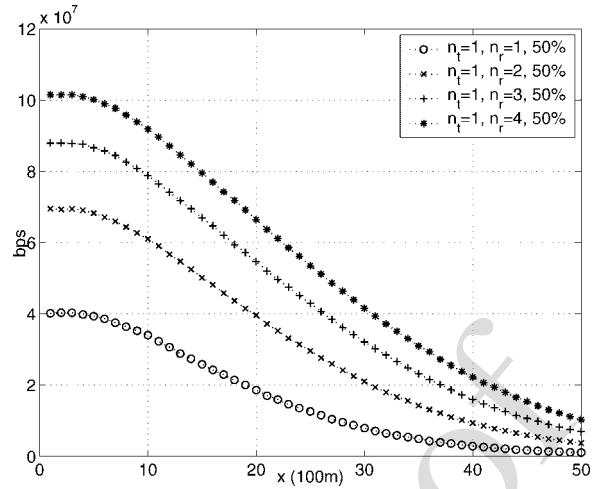


Fig. 11. Downlink average data rate of a receive diversity only system along the x-axis.

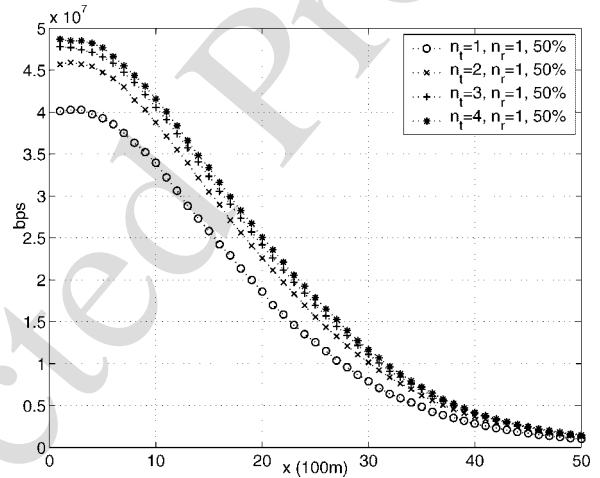


Fig. 12. Downlink average data rate of a transmit diversity only system along the x-axis.

assumption, transmit diversity will only weaken the signal quality of the MEA subchannels, resulting in lower data rates. However, transmit diversity indeed improves the average data rate for a system which does not employ receive diversity.

5. Conclusions

This paper presents an analysis of wireless high-speed data services for cellular CDMA systems. Numerical results are presented for the cell with two-tier interfering cells. Uniform user distribution is assumed. Users are allocated with either full system resources (i.e., all multicode channels) or minimal system

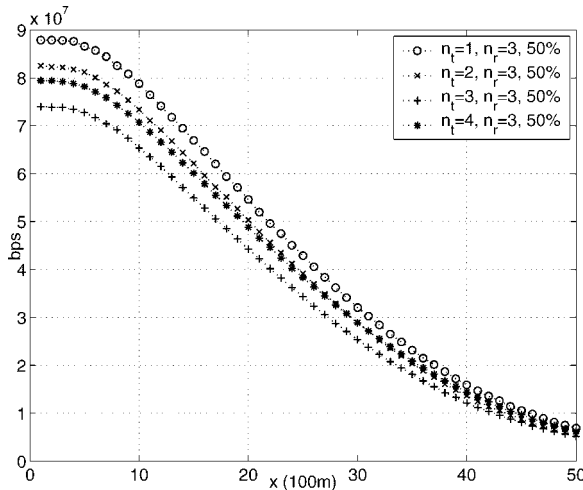


Fig. 13. Downlink average data rate of a transmit diversity system ($n_r = 3$).

resources (i.e., one multicode channel). Coverage maps, peak data rate, peak throughput, average throughput, peak spectral efficiency, and average spectral efficiency are obtained for the three ITU-R M.1225 test environments. It is shown that a data user with all the system resources performs better in the vehicular channel than in the outdoor to indoor pedestrian channel. Multicode allocation and its impact on average data rate is also investigated. It is shown that doubling the number of multicodes allocated to a user will result in more than doubling the achievable average data rate. Different antenna configurations are investigated. It is shown that the benefit of deploying transmit diversity is not as good as deploying receiver diversity. In most cases, simple one transmitting antenna configuration achieves the best data rate provided by the wireless channel.

Acknowledgment

The authors thank Dragan Nerandzic for his support and help in this research.

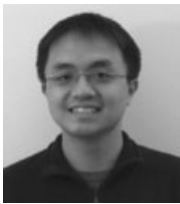
References

- Coffman KG, Odlyzko AM. Internet growth: Is there a "Moore's Law" for data traffic? In *Handbook of Massive Data Sets*, Abello J, Pardalos PM, Resende MGC (eds). Kluwer, 2002; 47–93. ^{Q3}
- Qualcomm Incorporated. White paper: The economics of wireless mobile data, 2001. <http://www.qualcomm.com/main/whitepapers/WirelessMobileData.pdf>.

- www.mobileGPRS.com. White paper: YES to GPRS, February 2001. <http://www.mobilewhitepapers.com/pdf/gprs.html>.
- Robinson M. Life on the edge. *Wireless Review* 2000; 17(18): 36–40.
- 3rd Generation Partnership Project 2. Physical Layer Standard for cdma2000 Spread Spectrum Systems Release 0, June 15, 2001. 3GPP2 C.S0002.
- Vanghi V, Damnjanovic A, Vojcic B. *The cdma2000 System for Mobile Communications*. Prentice Hall, 2004. ^{Q3}
- 3rd Generation Partnership Project 2. *cdma2000 High Rate Packet Data Air Interface Specification Ver 4.0*, 25 October 2002. 3GPP2 C.S0024.
- 3rd Generation Partnership Project 2. Physical Layer Standard for cdma2000 Spread Spectrum Systems Release D, 13 February 2004. 3GPP2 C.S0002-D.
- 3rd Generation Partnership Project Technical Specification Group Radio Access Network. Physical Channels and Mapping of Transport Channels onto Physical Channels (FDD) Release 5 September 2004. 3GPP TS 25.211 V5.6.0.
- Foschini GJ, Gans MJ. On limits of wireless communications in a fading environment when using multiple antennas. *Wireless Personal Communications* 1998; 311–355. ^{Q4}
- Foschini GJ. Layered space-time architecture for wireless communication in a fading environment when using multiple-element antennas. *Bell Labs Technical Journal* 1996; 41–59. ^{Q4}
- Chuah C-N, Tse DN, Kahn JM, Velenzuela RA. Capacity scaling in MIMO wireless systems under correlated fading. *IEEE Transactions on Information Theory* 2002; 48(3): 637–650.
- Holtzman JM. CDMA forward link waterfilling power control. In *Proceedings of 2000 IEEE Vehicular Technology Conference* 1663–1667. ^{Q5}
- Shiu D-S, Forchini GJ, Gans MJ, Kahn JM. Fading correlation and its effect on the capacity of multielement antenna systems. *IEEE Transactions on Communications* 2000; 48(3): 502–513.
- Wang H, Bu Z, Lilleberg J. Multiple-input single-output precoder for WCDMA TDD downlink transmission. In *Proceedings of 54th IEEE Vehicular Technology Conference* 2001; 581–585. ^{Q4}
- Gore D, Naber R, Paulraj A. Selecting an optimal set of transmit antennas for a low rank matrix channel. In *Proceedings of 2000 IEEE International Conference on Acoustics, Speech, and Signal Processing* 2000; 2785–2788. ^{Q6}
- I C-L^{Q6}, Gitlin RD. Multi-code CDMA wireless personal communications networks. In *Proceedings of IEEE International Conference on Communications (ICC)* 1995; 2: pp. 1060–1064.
- Soong ACK, Oh S-J, Damnjanovic A, Yoon YC. Forward high-speed wireless packet data service in IS-2000-1xEV-DV. *IEEE Communication Magazine* 2003; 41(8): 170–177.
- Liu X, Chong EKP, Shroff NB. Transmission scheduling for efficient wireless utilization. In *Proceedings of IEEE/ACM INFOCOM* 2000; 2: 776–785.
- Jakes W (ed.). *Microwave Mobile Communication*. Wiley, 1974. ^{Q3}
- I. T. U. R. Sector. *Recommendation ITU-R M.1225 Guidelines for evaluation of radio transmission technologies for IMT-2000*, 1998.
- 3GPP-3GPP2 Spatial Channel Model Ad-Hoc Group, *Spatial Channel Model Text Description*, 22 April 2003. version 6.0.
- 3GPP2 TSG-C WG3. *1xEV-DV Evaluation Methodology—Addendum (V14)*. 3GPP2 Contribution C30-20030616-043R1, 16 June 2003.
- Brenna D. Linear diversity combining techniques. In *Proceedings of IRE* 1959; 47.
- Mark JM, Zhuang W. *Wireless Communications and Networking*. Prentice Hall: Upper Saddle River, New Jersey, 2003. ^{Q3}

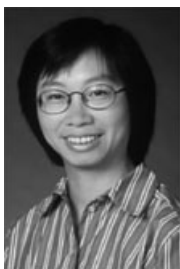
26. Ayyagari D, Ephremides A. Cellular multicode CDMA capacity for integrated (voice and data) services. *IEEE Transactions on Selected Areas in Communications* 1999; **17**(5): 928–938.
27. Lee JS, Miller LE. *CDMA Systems Engineering Handbook* (1st edn). Artech House, 1998.^{Q3}
28. Jalali A, Gutierrez A. Performance comparison of direct spread and multicarrier CDMA systems. In *Proceedings of 1998 IEEE Vehicular Technology Conference* 1998: 2042–2046.^{Q4}
29. Cardieri P, Rappaport TS. Statistics of the sum of lognormal variables in wireless communications. In *Proceedings of IEEE Vehicular Technology Conference* 2000: 1823–1827.^{Q4}
30. Choi W, Kang BS, Lee JC, Lee KT. Forward link Erlang capacity of 3G CDMA system. In *Proceedings of 1st International Conference on 3G Mobile Communication Technologies* 2000; pp. 213–217.
31. Zhou J, Yamamoto U, Onozato Y. On the feasibility of high data rate services in wireless system using code division multiple access. *IEICE Transactions Fundamentals* 2000; **E83-A**(7): 1347–1355.
32. Yoon YC. An improved Gaussian approximation for probability of bit-error analysis of asynchronous bandlimited DS-SSMA systems with BPSK spreading. *IEEE Transactions on Wireless Communication* 2002; **1**: 373–382. Q3
33. Gao W, Cho JH, Lehnert JS. Chip waveform design for DS-SSMA systems with aperiodic random spreading sequences. *IEEE Transactions on Wireless Communication* 2002; **1**(1): 37–45. Q4
34. Lee EA, Messerschmitt DG. *Digital Communication* (2nd edn). Kluwer: Norwell, MA, 1994. Q4

Authors' Biographies



Kevin K. H. Chan received his B.A.Sc. degree with first class honor in Electrical Engineering (Computer Engineering option) and M.A.Sc. degree in Electrical Engineering both from the University of Waterloo, Canada in 2000 and 2003, respectively. From 1999 to 2000, he was a research assistant with the Centre for Wireless

Communications at the University of Waterloo, Canada. His research interests were in third-generation CDMA high-speed data services and their evolution. From 2000 to 2001, he was a research contractor with the Technology Planning group of Bell Mobility cellular where he accomplished a comparative analysis of emerging third-generation wireless high-speed data services. From 2001 to 2003, he was a senior corporate application engineer with the System Level Design group of Synopsys, Inc. He is presently an engineer with Qualcomm CDMA Technologies, San Diego, California, doing performance testing of Qualcomm's Mobile Station Modem (MSMTM) chipsets. His research interests are in the design and analysis of the physical layer of CDMA systems as well as in CDMA standard evolution. He received the Industrial Postgraduate Scholarship Award and the Undergraduate Student Research Award from the Canadian National Science and Engineering Research Council (NSERC) in 2000 and 1999, respectively.



Weihua Zhuang received her B.Sc. and M.Sc. degrees from Dalian Maritime University, China, and the Ph.D. from the University of New Brunswick, Canada, all in Electrical Engineering. Since October 1993, she has been with the Department of Electrical and Computer Engineering, University of Waterloo, ON, Canada, where she is a full professor. She was a visiting professor at the Department of Information

Engineering, the Chinese University of Hong Kong, from August 2003 to June 2004. She is a co-author of the textbook *Wireless Communications and Networking* (Prentice Hall, 2003). Her current research interests include multimedia wireless communications, wireless networks, and radio

positioning. Dr Zhuang received the Premier's Research Excellence Award (PREA) in 2001 from the Ontario Government for demonstrated excellence of scientific and academic contributions. She is an associate editor of *IEEE Transactions on Vehicular Technology* and *EURASIP Journal on Wireless Communications and Networking*. She is a licensed professional engineer in the Province of Ontario, Canada.



Young C. Yoon received his B.A.Sc. degree in Engineering Science (Electrical option) from the University of Toronto, Canada, in 1989, the Masters degree in Electrical Engineering from Yokohama National University, Japan, in 1993, and the Ph.D. in Electrical Engineering from McGill University, Montreal, Canada, in 1998. From 1996

to 1997, he was a research assistant with the Telecommunications and Signal Processing Laboratory at McGill. From 1998 to 2001, he was an assistant professor with the Department of Electrical and Computer Engineering and Centre for Wireless Communications at the University of Waterloo, Canada. He was a co-recipient of the Telecom System Technology Prize from the Telecommunication Advancement Foundation, Japan, in 1995 for contributions to interference cancellation techniques in CDMA systems. He was a visiting researcher with the Advanced Telecommunications Laboratory, SONY Computer Sciences Laboratory, Japan, Fall 2000 and a visiting researcher with Ericsson Research, Sweden Spring 2002. Dr Yoon joined Ericsson Research at Ericsson Wireless Communications, San Diego, USA in 2001 and is presently a senior staff engineer with CDMA Radio Access Networks, System Engineering. He has authored or co-authored over 40 published papers and has over 20 patents granted or pending. His interests are in advanced receiver design, air-interface standards development, CDMA system design, and performance analysis. He is a senior member of the IEEE, serves as an associate editor for the *IEEE Transactions on Vehicular Technology*, a technical reviewer for *IEEE journals in communications*, and has served as a guest editor for *IEEE Communications Magazine* and a Technical Program Committee member for *IEEE conferences in communications*.

1
2
3
4
5
6 **Author Query Form (WCM/293)**
7
8

9 **Special Instructions: Author please write responses to queries directly on Galley proofs**
10 **and then fax back. Alternatively please list responses in an e-mail.**
11
12

13 **Q1: Author: Please check the suitability of**
14 **short title.**

15 **Q2: Author: Please check the insertion of**
16 **curly bracket, is it OK?**

17 **Q3: Author: Please provide publishing**
18 **location.**

19 **Q4: Author: Please provide volume no.**

20 **Q5: Author: Please provide year and**
21 **volume no.**

22 **Q6: Author: Please check author name.**

23 **Q7: Author: Please check the quality of**
24 **Figure.**
25
26
27
28
29
30
31
32
33
34
35
36
37
38
39
40
41
42
43
44
45
46
47
48
49
50
51
52
53
54
55
56
57
58
59